

DISKS THAT ARE DOUBLE SPIRAL STAIRCASES

TOBIAS H. COLDING AND WILLIAM P. MINICOZZI II

What are the possible shapes of various things and why?

For instance, when a closed wire or a frame is dipped into a soap solution and is raised up from the solution, the surface spanning the wire is a soap film; see p. 11 of [Op] or fig. I that show a soap film with the shape of a (single) spiral staircase. What are the possible shapes of soap films and why? Or, for instance, why is DNA like a double spiral staircase? “What..?” and “why..?” are fundamental questions, and when answered, help us understand the world we live in.

Soap films, soap bubbles, and surface tension were extensively studied by the Belgian physicist and inventor (the inventor of the stroboscope) Joseph Plateau in the first half of the nineteenth century. At least since his studies, it has been known that the right mathematical model for soap films are minimal surfaces – the soap film is in a state of minimum energy when it is covering the least possible amount of area.

We will discuss here the answer to the question: “What are the possible shapes of embedded minimal disks in \mathbf{R}^3 and why?”.

The field of minimal surfaces dates back to the publication in 1762 of Lagrange’s famous memoir “Essai d’une nouvelle méthode pour déterminer les maxima et les minima des formules intégrales indéfinies”. Euler had already in a paper published in 1744 discussed minimizing properties of the surface now known as the catenoid, but he only considered variations within a certain class of surfaces. In the almost one quarter of a millenium that has past since Lagrange’s memoir minimal surfaces has remained a vibrant area of research and there are many reasons why. The study of minimal surfaces was the birthplace of regularity theory. It lies on the intersection of nonlinear elliptic PDE, geometry, and low-dimensional topology and over the years the field has matured through the efforts of many people. However some very fundamental questions remain. Moreover, many of the potentially spectacular applications of the field have yet to be achieved. For instance, it has long been the hope that several of the outstanding conjectures about the topology of 3-manifolds could be resolved using detailed knowledge of minimal surfaces. Surfaces with uniform curvature (or area) bounds have been well understood and the regularity theory is complete, yet essentially nothing was known without such bounds. We discuss here the theory of embedded minimal disks in \mathbf{R}^3 without a priori bounds. As we will see, the helicoid, which is a double spiral staircase, is the most important example of such a disk. In fact, we will see that every embedded minimal disk is either a graph of a function or is part of a double spiral staircase. The helicoid was discovered to be a minimal surface by Meusnier in 1776.

The authors were partially supported by NSF Grants DMS 0104453 and DMS 0104187.

Double spiral staircases

A *double spiral staircase* consists of two staircases that spiral around one another so that without meeting two people can pass each other. For instance, one could ascend one staircase while the other descends the other staircase. Fig. II

(<http://www.a-castle-for-rent.com/castles/images/Chambord14.jpg>)

shows Leonardo da Vinci's double spiral staircase in Château de Chambord in the Loire valley in France. The construction of the castle began in 1519 (the same year that Leonardo da Vinci died) and was completed in 1539. Fig. III

(<http://www.angelfire.com/trek/lafrance1999/tours3.html>)

show a model of the double spiral staircase where we can clearly see the two staircases spiraling around one another. In fig. IV

(<http://images.amazon.com/images/P/0451627873.01.LZZZZZZZ.jpg>)

we see “the double helix” which was discovered in 1952 by Crick and Watson to be the structure of DNA. The double spiral structure represented the culmination of half a century of prior work on genetics and is by many considered one of the greatest scientific discoveries of the twentieth century. Also the internal ear, the cochlea, is a double spiral staircase; see fig. V or p. 343 of [K].

In the cochlea, the two canals wind around a conical bony axis and after about two and a half rotations they meet at the top and fuse. The canals are filled with fluids and sound waves travel up one canal, turn around, and come down the other. When the liquid is set into movement, it will set the Basilar membrane and the hair cells into vibration. Different hair cells correspond to different frequencies.

Other examples of double spiral staircases include parking ramps.

What is a minimal surface and what are the central examples?

Let $\Sigma \subset \mathbf{R}^3$ be a smooth orientable surface (possibly with boundary) with unit normal \mathbf{n}_Σ . Given a function ϕ in the space $C_0^\infty(\Sigma)$ of infinitely differentiable (i.e., smooth), compactly supported functions on Σ , consider the one-parameter variation

$$\Sigma_{t,\phi} = \{x + t\phi(x)\mathbf{n}_\Sigma(x) | x \in \Sigma\}. \quad (1)$$

The so called first variation formula of area is the equation (integration is with respect to $d\text{area}$)

$$\left. \frac{d}{dt} \right|_{t=0} \text{Area}(\Sigma_{t,\phi}) = \int_\Sigma \phi H, \quad (2)$$

where H is the mean curvature of Σ . (When Σ is noncompact, then $\Sigma_{t,\phi}$ in (2) is replaced by $\Gamma_{t,\phi}$, where Γ is any compact set containing the support of ϕ .) The surface Σ is said to be a *minimal* surface (or just minimal) if

$$\left. \frac{d}{dt} \right|_{t=0} \text{Area}(\Sigma_{t,\phi}) = 0 \quad \text{for all } \phi \in C_0^\infty(\Sigma) \quad (3)$$

or, equivalently by (2), if the mean curvature H is identically zero. Thus Σ is minimal if and only if it is a critical point for the area functional. (Since a critical point is not necessarily a minimum the term “minimal” is misleading, but it is time honored. The equation for a critical point is also sometimes called the Euler-Lagrange equation.) Moreover, a computation shows

that if Σ is minimal, then

$$\left. \frac{d^2}{dt^2} \right|_{t=0} \text{Area}(\Sigma_{t,\phi}) = - \int_{\Sigma} \phi L_{\Sigma} \phi, \quad \text{where } L_{\Sigma} \phi = \Delta_{\Sigma} \phi + |A|^2 \phi \quad (4)$$

is the second variational (or Jacobi) operator. Here Δ_{Σ} is the Laplacian on Σ and A is the second fundamental form. So $|A|^2 = \kappa_1^2 + \kappa_2^2$, where κ_1, κ_2 are the principal curvatures of Σ and $H = \kappa_1 + \kappa_2$. A minimal surface Σ is said to be stable if

$$\left. \frac{d^2}{dt^2} \right|_{t=0} \text{Area}(\Sigma_{t,\phi}) \geq 0 \quad \text{for all } \phi \in C_0^{\infty}(\Sigma). \quad (5)$$

One can show that a minimal graph is stable and, more generally, so is a multi-valued minimal graph (see below for the precise definition).

There are two local models for embedded minimal disks (by an *embedded disk* we mean a smooth injective map from the closed unit ball in \mathbf{R}^2 into \mathbf{R}^3). One model is the plane (or, more generally, a minimal graph) and the other is a piece of a helicoid.

The derivation of the equation for a minimal graph goes back to Lagrange's 1762 memoir.

Example 1: (Minimal graphs). If Ω is a simply connected domain in \mathbf{R}^2 and u is a real valued function on Ω satisfying the minimal surface equation

$$\text{div} \left(\frac{\nabla u}{\sqrt{1 + |\nabla u|^2}} \right) = 0, \quad (6)$$

then the graph of u , i.e., the set $\{(x_1, x_2, u(x_1, x_2)) \mid (x_1, x_2) \in \Omega\}$, is a minimal disk.

A classical theorem of Bernstein from 1916 says that entire (i.e., where $\Omega = \mathbf{R}^2$) minimal graphs are planes. This remarkable theorem of Bernstein was one of the first illustrations of the fact that the solutions to a nonlinear PDE, like the minimal surface equation, can behave quite differently from the solutions to a linear equation. In the early nineteen-eighties Schoen and Simon extended the theorem of Bernstein to complete simply connected embedded minimal surfaces in \mathbf{R}^3 with quadratic area growth. A surface Σ is said to have quadratic area growth if for all $r > 0$, the intersection of the surface with the ball in \mathbf{R}^3 of radius r and center at the origin is bounded by $C r^2$ for a fixed constant C independent of r .

The second model comes from the helicoid which was discovered by Meusnier in 1776. Meusnier had been a student of Monge. He also discovered that the surface now known as the catenoid is minimal in the sense of Lagrange, and he was the first to characterize a minimal surface as a surface with vanishing mean curvature. Unlike the helicoid, the catenoid is not topologically a plane but rather a cylinder.

The helicoid is a "double spiral staircase".

Example 2: (Helicoid; see fig. 1). The helicoid is the minimal surface in \mathbf{R}^3 given by the parametrization

$$(s \cos t, s \sin t, t), \quad \text{where } s, t \in \mathbf{R}. \quad (7)$$

To be able to give a precise meaning to the statement that the helicoid is a double spiral staircase we will need the notion of a multi-valued graph, each staircase will be a multi-valued graph, see fig. 1. Intuitively, an (embedded) multi-valued graph is a surface such that over each point of the annulus, the surface consists of N graphs. To make this notion

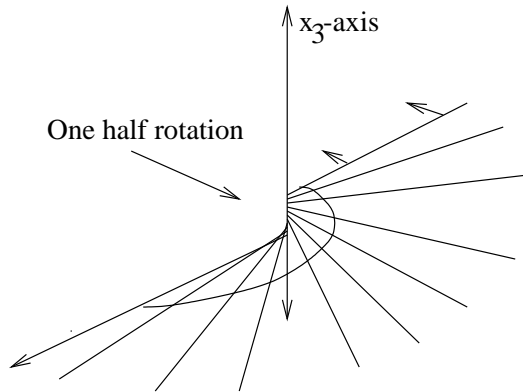


FIGURE 1. Multi-valued graphs. The helicoid is obtained by gluing together two ∞ -valued graphs along a line.

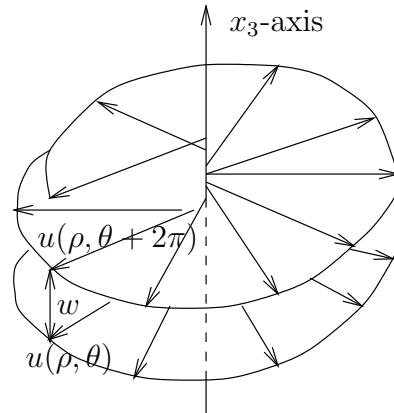


FIGURE 2. The separation w grows/decays in ρ at most sub-linearly for a multi-valued minimal graph; see (12).

precise, let D_r be the disk in the plane centered at the origin and of radius r and let \mathcal{P} be the universal cover of the punctured plane $\mathbf{C} \setminus \{0\}$ with global polar coordinates (ρ, θ) so $\rho > 0$ and $\theta \in \mathbf{R}$. An N -valued graph on the annulus $D_s \setminus D_r$ is a single valued graph of a function u over $\{(\rho, \theta) \mid r < \rho \leq s, |\theta| \leq N\pi\}$. For working purposes, we generally think of the intuitive picture of a multi-sheeted surface in \mathbf{R}^3 , and we identify the single-valued graph over the universal cover with its multi-valued image in \mathbf{R}^3 .

The multi-valued graphs that we will consider will all be embedded, which corresponds to a nonvanishing separation between the sheets (or the floors). Here the *separation* is the function (see fig. 2)

$$w(\rho, \theta) = u(\rho, \theta + 2\pi) - u(\rho, \theta). \quad (8)$$

If Σ is the helicoid, then $\Sigma \setminus \{x_3 - \text{axis}\} = \Sigma_1 \cup \Sigma_2$, where Σ_1, Σ_2 are ∞ -valued graphs on $\mathbf{C} \setminus \{0\}$. Σ_1 is the graph of the function $u_1(\rho, \theta) = \theta$ and Σ_2 is the graph of the function $u_2(\rho, \theta) = \theta + \pi$. (Σ_1 is the subset where $s > 0$ in (7) and Σ_2 the subset where $s < 0$.) In either case the separation $w = 2\pi$. A *multi-valued minimal graph* is a multi-valued graph of a function u satisfying the minimal surface equation.

Note that for an embedded multi-valued graph, the sign of w determines whether the multi-valued graph spirals in a left-handed or right-handed manner, in other words, whether upwards motion corresponds to turning in a clockwise direction or in a counterclockwise direction. For DNA, although both spirals occur, the right-handed spiral is far more common because of certain details of the chemical structure; see [CaDr].

As we will see, a fundamental theorem about embedded minimal disks is that such a disk is either a minimal graph or can be approximated by a piece of a rescaled helicoid depending on whether the curvature is small or not; see Theorem 1 below. To avoid tedious dependence of various quantities we state this, our main result, not for a single embedded minimal disk with sufficiently large curvature at a given point but instead for a sequence of such disks where the curvatures are blowing up. Theorem 1 says that a sequence of embedded minimal disks mimics the following behavior of a sequence of rescaled helicoids.

Consider the sequence $\Sigma_i = a_i \Sigma$ of rescaled helicoids where $a_i \rightarrow 0$. (That is, rescale \mathbf{R}^3 by a_i , so points that used to be distance d apart will in the rescaled \mathbf{R}^3 be distance $a_i d$ apart.) The curvatures of this sequence of rescaled helicoids are blowing up along the vertical axis. The sequence converges (away from the vertical axis) to a foliation by flat parallel planes. The singular set \mathcal{S} (the axis) then consists of removable singularities.

Throughout let x_1, x_2, x_3 be the standard coordinates on \mathbf{R}^3 . For $y \in \Sigma \subset \mathbf{R}^3$ and $s > 0$, the extrinsic and intrinsic balls are $B_s(y)$, $\mathcal{B}_s(y)$. That is, $B_s(y) = \{x \in \mathbf{R}^3 \mid |x - y| < s\}$ and $\mathcal{B}_s(y) = \{x \in \Sigma \mid \text{dist}_\Sigma(x, y) < s\}$. $K_\Sigma = \kappa_1 \kappa_2$ is the Gaussian curvature of $\Sigma \subset \mathbf{R}^3$, so when Σ is minimal (i.e., $\kappa_1 = -\kappa_2$), then $|A|^2 = -2K_\Sigma$.

See [CM1], [O], [S] (and the forthcoming book [CM3]) for background and basic properties of minimal surfaces and [CM2] for a more detailed survey of the results described here and references. See also [C] for an abbreviated version of this paper intended for a general non-mathematical audience. The article [A] discusses in a simple nontechnical way the shape of various things that are of “minimal” type. These shapes include soap films and soap bubbles, metal alloys, radiolarian skeletons, and embryonic tissues and cells. The reader interested in some of the history of the field of minimal surfaces may consult [DHKW], [N], and [T].

The limit foliation and the singular curve

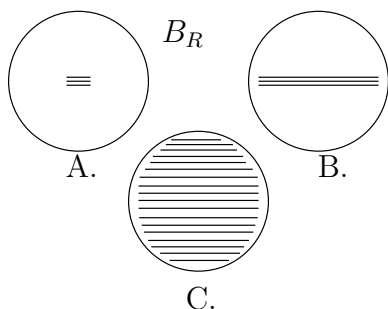


FIGURE 3. Proving Theorem 1. A. Finding a small N -valued graph in Σ . B. Extending it in Σ to a large N -valued graph. C. Extending the number of sheets.

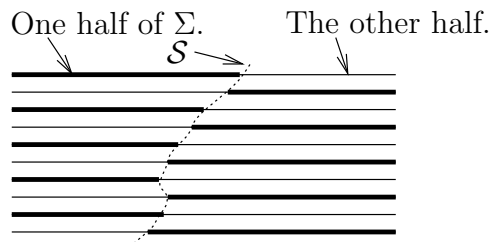


FIGURE 4. Theorem 1 - the singular set and the two multi-valued graphs.

In the next few sections we will discuss how to show that every embedded minimal disk is either a graph of a function or part of a double spiral staircase; Theorem 1 below gives precise meaning to this statement. In particular, we will in the next few sections discuss the following; see fig. 3:

A. Fix an integer N (the “large” of the curvature in what follows will depend on N). If an embedded minimal disk Σ is not a graph (or equivalently if the curvature is large at some point), then it contains an N -valued minimal graph which initially is shown to exist on the scale of $1/\max|A|$. That is, the N -valued graph is initially shown to be defined on an annulus with both inner and outer radius inversely proportional to $\max|A|$.

B. Such a potentially small N -valued graph sitting inside Σ can then be seen to extend as an N -valued graph inside Σ almost all the way to the boundary. That is, the small N -valued graph can be extended to an N -valued graph defined on an annulus where the outer radius of the annulus is proportional to R . Here R is the radius of the ball in \mathbf{R}^3 that the boundary of Σ is contained in.

C. The N -valued graph not only extends horizontally (i.e., tangent to the initial sheets) but also vertically (i.e., transversally to the sheets). That is, once there are N sheets there are many more and, in fact, the disk Σ consists of two multi-valued graphs glued together along an axis.

These three items, A., B., and C. will be used to demonstrate the following theorem, which is the main result:

Theorem 1. (See fig. 4). Let $\Sigma_i \subset B_{R_i} = B_{R_i}(0) \subset \mathbf{R}^3$ be a sequence of embedded minimal disks with $\partial\Sigma_i \subset \partial B_{R_i}$ where $R_i \rightarrow \infty$. If $\sup_{B_1 \cap \Sigma_i} |A|^2 \rightarrow \infty$, then there exists a subsequence, Σ_j , and a Lipschitz curve $\mathcal{S} : \mathbf{R} \rightarrow \mathbf{R}^3$ such that after a rotation of \mathbf{R}^3 :

1. $x_3(\mathcal{S}(t)) = t$. (That is, \mathcal{S} is a graph over the x_3 -axis.)

2. Each Σ_j consists of exactly two multi-valued graphs away from \mathcal{S} (which spiral together).

3. For each $\alpha > 0$, $\Sigma_j \setminus \mathcal{S}$ converges in the C^α -topology to the foliation, $\mathcal{F} = \{x_3 = t\}_t$, of \mathbf{R}^3 by flat parallel planes.

4. $\sup_{B_r(\mathcal{S}(t)) \cap \Sigma_j} |A|^2 \rightarrow \infty$ for all $r > 0$, $t \in \mathbf{R}$. (The curvature blows up along \mathcal{S} .)

In 2., 3. the statement that $\Sigma_j \setminus \mathcal{S}$ are multi-valued graphs and converge to \mathcal{F} means that for each compact subset $K \subset \mathbf{R}^3 \setminus \mathcal{S}$ and j sufficiently large $K \cap \Sigma_j$ consists of multi-valued graphs over (part of) $\{x_3 = 0\}$ and $K \cap \Sigma_j \rightarrow K \cap \mathcal{F}$.

As will be clear in the following sections, A., B., and C. alone are not enough to prove Theorem 1. For instance, 1. does not follow from A., B., and C. but needs a more precise statement than C. of where the new sheets form above and below a given multi-valued graph. This is done using the ‘‘one-sided curvature estimate’’.

Here is a summary of the rest of the paper:

First we discuss two key results that are used in the proof of Theorem 1. These are the existence of multi-valued graphs, i.e., A. and B., and the important one-sided curvature estimate. Following that we discuss some bounds for the separation of multi-valued minimal graphs. These bounds are used in both B. and C. above and we discuss what they are used for in C. After that we explain how the one-sided curvature estimate is used to show that the singular set, \mathcal{S} , is a Lipschitz curve. The two last sections before our concluding remarks contain further discussion on the existence of multi-valued graphs and on the proof of the one-sided curvature estimate.

Two key ingredients in the proof of Theorem 1 - Existence of multi-valued graphs and the one-sided curvature estimate

We now come to the two key results about embedded minimal disks. The first says that if the curvature of such a disk Σ is large at some point $x \in \Sigma$, then near x a multi-valued graph forms (in Σ) and this extends (in Σ) almost all the way to the boundary. Moreover, the inner radius, r_x , of the annulus where the multi-valued graphs is defined is inversely proportional

to $|A|(x)$ and the initial separation between the sheets is bounded by a constant times the inner radius, i.e., $|w(r_x, \theta)| \leq C r_x$.

An important ingredient in the proof of Theorem 1 is that, just like the helicoid, general embedded minimal disks with large curvature at some interior point can be built out of N -valued graphs. In other words, any embedded minimal disk can be divided into pieces each of which is an N -valued graph. Thus the disk itself should be thought of as being obtained by stacking these pieces (graphs) on top of each other.

The second key result (Theorem 2) is a curvature estimate for embedded minimal disks in a half-space. As a corollary of this theorem, we get that the set of points in an embedded minimal disk where the curvature is large lies within a cone and thus the multi-valued graphs, whose existence were discussed above, will all start off within this cone; see fig. 8 and fig. 9.

The curvature estimate for disks in a half-space is the following:

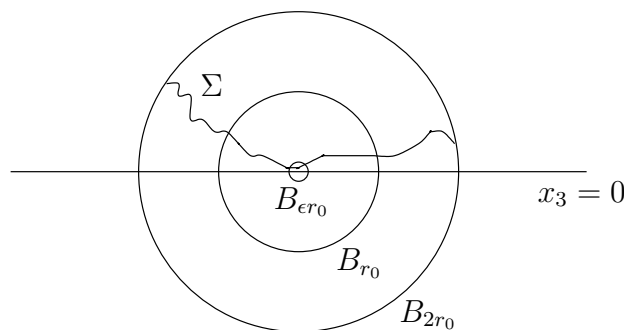


FIGURE 5. The one-sided curvature estimate for an embedded minimal disk Σ in a half-space with $\partial\Sigma \subset \partial B_{2r_0}$: The components of $B_{r_0} \cap \Sigma$ intersecting $B_{\epsilon r_0}$ are graphs.

Theorem 2. (See fig. 5). There exists $\epsilon > 0$, such that for all $r_0 > 0$ if $\Sigma \subset B_{2r_0} \cap \{x_3 > 0\} \subset \mathbf{R}^3$ is an embedded minimal disk with $\partial\Sigma \subset \partial B_{2r_0}$, then for all components Σ' of $B_{r_0} \cap \Sigma$ which intersect $B_{\epsilon r_0}$

$$\sup_{x \in \Sigma'} |A_\Sigma(x)|^2 \leq r_0^{-2}. \quad (9)$$

Theorem 2 is an interior estimate where the curvature bound, (9), is on the ball B_{r_0} of one half of the radius of the ball B_{2r_0} that Σ is contained in. This is just like a gradient estimate for a harmonic function where the gradient bound is on one half of the ball where the function is defined.

Using the minimal surface equation and the fact that Σ' has points close to a plane, it is not hard to see that, for $\epsilon > 0$ sufficiently small, (9) is equivalent to the statement that Σ' is a graph over the plane $\{x_3 = 0\}$.

We will often refer to Theorem 2 as *the one-sided curvature estimate* (since Σ is assumed to lie on one side of a plane). Note that the assumption in Theorem 2 that Σ is simply connected (i.e., that Σ is a disk) is crucial as can be seen from the example of a rescaled catenoid. The catenoid, see fig. 6, is the minimal surface in \mathbf{R}^3 given by $(\cosh s \cos t, \cosh s \sin t, s)$ where $s, t \in \mathbf{R}$. Rescaled catenoids converge (with multiplicity two) to the flat plane; see fig. 7.

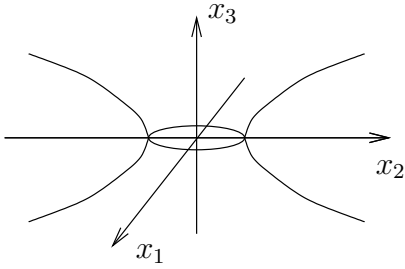


FIGURE 6. The catenoid given by revolving $x_1 = \cosh x_3$ around the x_3 -axis.

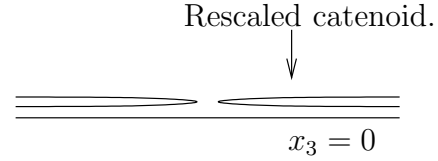


FIGURE 7. Rescaling the catenoid shows that the property of being simply connected (and embedded) is needed in the one-sided curvature estimate.

Likewise, by considering the universal cover of the catenoid, one sees that Theorem 2 requires the disk to be embedded, and not just immersed.

Definition 1. (Cones; see fig. 8). If $\delta > 0$ and $x \in \mathbf{R}^3$, then we denote by $\mathbf{C}_\delta(x)$ the (convex) cone with vertex x , cone angle $(\pi/2 - \arctan \delta)$, and axis parallel to the x_3 -axis. That is, (see fig. 8)

$$\mathbf{C}_\delta(x) = \{x \in \mathbf{R}^3 \mid x_3^2 \geq \delta^2 (x_1^2 + x_2^2)\} + x. \quad (10)$$

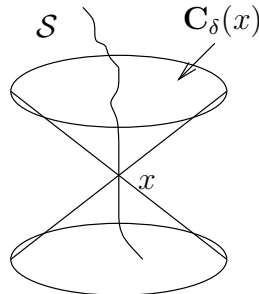


FIGURE 8. It follows from the one-sided curvature estimate that the singular set has the cone property and hence is a Lipschitz curve.

In the proof of Theorem 1, the following (direct) consequence of Theorem 2 (with Σ_d playing the role of the plane $\{x_3 = 0\}$, see fig. 9) is needed (Paraphrased, this corollary says that if an embedded minimal disk contains a 2-valued graph, then the disk consists of multi-valued graphs away from a cone with axis orthogonal to the 2-valued graph. In Corollary 1 the “d” in Σ_d stands for double-valued.):

Corollary 1. (See fig. 9). There exists $\delta_0 > 0$ so for all $r_0, R > 0$ with $r_0 < R$ if $\Sigma \subset B_{2R}$, $\partial\Sigma \subset \partial B_{2R}$ is an embedded minimal disk containing a 2-valued graph $\Sigma_d \subset \mathbf{R}^3 \setminus \mathbf{C}_{\delta_0}(0)$ over the annulus $D_R \setminus D_{r_0}$ with gradient $\leq \delta_0$, then each component of $B_{R/2} \cap \Sigma \setminus (\mathbf{C}_{\delta_0}(0) \cup B_{2r_0})$ is a multi-valued graph.

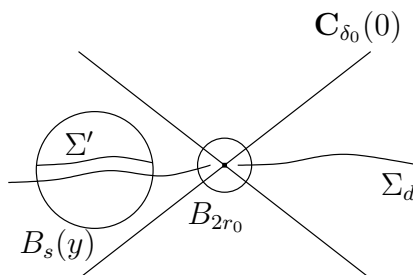


FIGURE 9. Corollary 1: With Σ_d playing the role of the plane $x_3 = 0$, by the one-sided estimate, Σ consists of multi-valued graphs away from a cone.

Fig. 9 illustrates how this corollary follows from Theorem 2. In this picture, $B_s(y)$ is a ball away from 0 and Σ' is a component of $B_s(y) \cap \Sigma$ disjoint from Σ_d . It follows easily from the maximum principle that Σ' is topologically a disk. Since Σ' is assumed to contain points near Σ_d , then we can let a component of $B_s(y) \cap \Sigma_d$ play the role of the plane $\{x_3 = 0\}$ in Theorem 2 and the corollary follows.

Using Theorems 1, 2, W. Meeks and H. Rosenberg proved in “The uniqueness of the helicoid and the asymptotic geometry of properly embedded minimal surfaces with finite topology” that the plane and helicoid are the only complete properly embedded simply-connected minimal surfaces in \mathbf{R}^3 . Catalan had proven in 1842 that any complete ruled minimal surface is either a plane or a helicoid. A surface is said to be *ruled* if it has the parametrization

$$X(s, t) = \beta(t) + s\delta(t), \quad \text{where } s, t \in \mathbf{R}, \quad (11)$$

and β, δ are curves in \mathbf{R}^3 . The curve $\beta(t)$ is called the *directrix* of the surface, and a line having $\delta(t)$ as direction vector is called a *ruling*. For the helicoid in (7), the x_3 -axis is a directrix, and for each fixed t the line $s \rightarrow (s \cos t, s \sin t, t)$ is a ruling.

Towards removability of singularities - Analysis of multi-valued minimal graphs

Even given the decomposition into multi-valued graphs mentioned in the beginning of the previous section, to prove Theorem 1, one still needs to analyze how the various N -valued pieces fit together. In particular, we need Theorem 2 and Corollary 1 to show that an embedded minimal disk that is not a graph cannot be contained in a half-space and thus the subset of points with large curvature lies within a cone. This is still not enough to imply Theorem 1. One also needs to show that part of any embedded minimal disk cannot accumulate in a half-space. This is what we call *properness* below; see fig. 10 and (14) that gives an example of an ∞ -valued graph whose image lies in a slab in \mathbf{R}^3 . The property we call properness is the assertion that no limit of embedded minimal disks can contain such a (nonproper) multi-valued graph.

In this section, we will discuss bounds for the separation of embedded multi-valued graphs and their applications to properness and to the proofs of Theorems 1, 2. Two types of bounds for the growth/decay (as $\rho \rightarrow \infty$) of the separation will be needed:

a. The weaker sublinear bounds, i.e., there exists $0 < \alpha < 1$ such that for fixed ρ_0 , we have the bounds

$$(\rho/\rho_0)^{-\alpha} |w(\rho_0, \theta)| \leq |w(\rho, \theta)| \leq (\rho/\rho_0)^\alpha |w(\rho_0, \theta)| \quad \text{as } \rho \rightarrow \infty. \quad (12)$$

These bounds hold for N -valued graphs (where N is some fixed large number). By letting N be large, α can be chosen small.

b. The stronger logarithmic bounds, i.e., there exist constants c_1 and c_2 such that for fixed ρ_0 , we have the bounds

$$\frac{c_1}{\log(\rho/\rho_0)} |w(\rho_0, \theta)| \leq |w(\rho, \theta)| \leq c_2 \log(\rho/\rho_0) |w(\rho_0, \theta)| \quad \text{as } \rho \rightarrow \infty. \quad (13)$$

These bounds will require a growing number of sheets (growing as $\rho \rightarrow \infty$) and will be used only to show properness; cf. fig. 10.

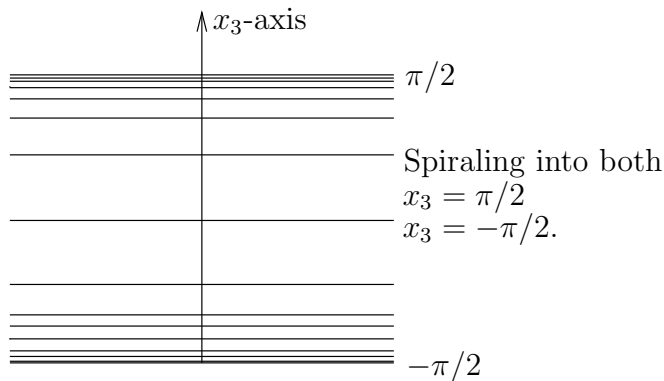


FIGURE 10. To show properness one needs to rule out that one of the multi-valued graphs can contain a nonproper graph like $\arctan(\theta/\log \rho)$, where (ρ, θ) are polar coordinates. The graph of $\arctan(\theta/\log \rho)$ is illustrated above.

Here are couple of things that the sublinear bounds are used for. First, as a consequence of the existence of multi-valued graphs discussed in the previous section, one easily gets that if $|A|^2$ is blowing up near 0 for a sequence of embedded minimal disks Σ_i , then there is a sequence of 2-valued graphs $\Sigma_{i,d} \subset \Sigma_i$. Here the 2-valued graphs start off defined on a smaller and smaller scale (the inner radius of the annulus where each multi-valued graph is defined is inversely proportional to $|A|$). Consequently, by the sublinear separation growth, such 2-valued graphs collapse: Namely, if $\Sigma_{i,d}$ is a 2-valued graph over $D_R \setminus D_{r_i}$, then $|w_i(\rho, \theta)| \leq (\rho/r_i)^\alpha |w_i(r_i, \theta)| \leq C \rho^\alpha r_i^{1-\alpha}$ for some $\alpha < 1$ and some constant C . (In fact, by making N large, α can be chosen small.) Letting $r_i \rightarrow 0$ shows that $|w_i(\rho, \theta)| \rightarrow 0$ for ρ, θ fixed. Thus as $i \rightarrow \infty$ the upper sheet collapses onto the lower and, hence, a subsequence converges to a smooth minimal graph through 0. (Here 0 is a removable singularity for the limit.) Moreover, if the sequence of such disks is as in Theorem 1, i.e., if $R_i \rightarrow \infty$, then the minimal graph in the limit is entire and hence, by Bernstein's theorem, is a plane.

The sublinear bounds are also used in the proof of Theorem 2 which in turn - through its corollary, Corollary 1 - is used to show that any multi-valued graph contained in an embedded minimal disk can be extended, inside the disk, to a multi-valued graph with a rapidly growing number of sheets and thus we get the better logarithmic bounds for the separation. Namely, by Corollary 1, outside a cone such a multi-valued graph extends as a multi-valued graph. An application of a Harnack inequality then shows that the number of sheets that it takes to leave the complement of the cone where the disk is graphical must grow in ρ sufficiently fast so that (13) follows. (Recall that for the bounds (13) to hold requires that the number of sheets grows sufficiently fast.)

By b. when the number of sheets grows sufficiently fast, the fastest possible decay for $w(\rho, 0)/w(1, 0)$ is $c_1/\log \rho$. This lower bound for the decay of the separation is sharp. It is achieved for the ∞ -valued graph of the harmonic function (graphs of multi-valued harmonic functions are good models for multi-valued minimal graphs)

$$u(\rho, \theta) = \arctan \frac{\theta}{\log \rho}. \quad (14)$$

Note that the graph of u is embedded and lies in a slab in \mathbf{R}^3 , i.e., $|u| \leq \pi/2$, and hence in particular is not proper. On the top it spirals into the plane $\{x_3 = \pi/2\}$ and on the bottom into $\{x_3 = -\pi/2\}$, yet it never reaches either of these planes; see fig. 10.

The next proposition rules out not only this as a possible limit of (one half of) embedded minimal disks, but, more generally, any ∞ -valued minimal graph in a half-space.

Proposition 1. Multi-valued graphs contained in embedded minimal disks are proper - they do not accumulate in finite height.

Proposition 1 relies in part on the logarithmic bound, (13), for the separation.

Regularity of the singular set and Theorem 1

In this section we will indicate how to define the singular set \mathcal{S} in Theorem 1 and show regularity of \mathcal{S} .

By a very general standard compactness argument, it follows (after possibly going to a subsequence) that for a sequence of smooth surfaces there is a well defined notion of points where the second fundamental form of the sequence blows up. That is, let $\Sigma_i \subset B_{R_i}$, $\partial\Sigma_i \subset \partial B_{R_i}$, and $R_i \rightarrow \infty$ be a sequence of (smooth) compact surfaces. After passing to a subsequence, Σ_j , we may assume that for each $x \in \mathbf{R}^3$ either (a) or (b) holds:

- (a) $\sup_{B_r(x) \cap \Sigma_j} |A|^2 \rightarrow \infty$ for all $r > 0$,
- (b) $\sup_j \sup_{B_r(x) \cap \Sigma_j} |A|^2 < \infty$ for some $r > 0$.

Definition 2. (Cone property). Fix $\delta > 0$. We will say that a subset $\mathcal{S} \subset \mathbf{R}^3$ has the *cone property* (or the δ -cone property) if \mathcal{S} is closed and nonempty and:

- (i) If $z \in \mathcal{S}$, then $\mathcal{S} \subset \mathbf{C}_\delta(z)$; see Definition 1 for $\mathbf{C}_\delta(z)$.
- (ii) If $t \in x_3(\mathcal{S})$ and $\epsilon > 0$, then $\mathcal{S} \cap \{t < x_3 < t + \epsilon\} \neq \emptyset$ and $\mathcal{S} \cap \{t - \epsilon < x_3 < t\} \neq \emptyset$.

Note that (ii) just says that each point in \mathcal{S} is the limit of points coming from above and below.

When $\Sigma_i \subset B_{R_i} \subset \mathbf{R}^3$ is a sequence of embedded minimal disks with $\partial\Sigma_i \subset \partial B_{R_i}$, $R_i \rightarrow \infty$, Σ_j is the subsequence as above, and \mathcal{S} is the set of points where the curvatures of Σ_j blow

up (i.e., where (a) above holds), then we will see below that \mathcal{S} has the cone property (after a rotation of \mathbf{R}^3). Hence (by the next lemma), \mathcal{S} is a Lipschitz curve which is a graph over the x_3 -axis. Note that when Σ_i is a sequence of rescaled helicoids, then \mathcal{S} is the x_3 -axis.

Lemma 1. (See fig. 8). If $\mathcal{S} \subset \mathbf{R}^3$ has the δ -cone property, then $\mathcal{S} \cap \{x_3 = t\}$ consists of exactly one point \mathcal{S}_t for all $t \in \mathbf{R}$, and $t \rightarrow \mathcal{S}_t$ is a Lipschitz parameterization of \mathcal{S} .

With Lemma 1 in hand, we can proceed with the proof of Theorem 1. So suppose that Σ_i is as in Theorem 1 and Σ_j , \mathcal{S} are as above, then \mathcal{S} is closed by definition and nonempty by the assumption of Theorem 1. Centered at any $x \in \mathcal{S}$ we can, by the existence of multi-valued graphs near points where the curvatures blow up, the sublinear separation growth, and Bernstein's theorem, find a sequence of 2-valued graphs $\Sigma_{d,j} \subset \Sigma_j$ which converges to a plane through x ; see the discussion preceding Theorem 2. (This is after possibly passing to a subsequence of the Σ_j 's.) Thus (i) above holds by Corollary 1. Therefore to see that \mathcal{S} has the cone property all we need to see is that (ii) holds. The proof of this relies on Proposition 1. Once the cone property of \mathcal{S} is shown, it follows from Lemma 1 that \mathcal{S} is a Lipschitz curve and by Corollary 1, away from \mathcal{S} , each Σ_j consists of multi-valued graphs. It is not hard to see that there are at least two such graphs and a barrier argument shows that there are not more.

Blow up points and the existence of multi-valued graphs

To describe the existence of multi-valued graphs in embedded minimal disks, we will need the notion of a blow up point.

Let Σ be a smooth (minimal or not) embedded (compact) surface in a ball $B_{r_0}(x)$ in \mathbf{R}^3 , passing through x the center of the ball, and with boundary contained in the boundary of the ball. Here $B_{r_0}(x)$ is the extrinsic ball of radius r_0 , but could as well have been an intrinsic ball $\mathcal{B}_{r_0}(x)$ in which case the notion of a blow up point below would have to be appropriately changed. Suppose that $|A|^2(x) \geq 4C^2 r_0^{-2}$ for some constant $C > 0$. We claim that there is $y \in B_{r_0}(x) \cap \Sigma$ and $s > 0$ such that $B_s(y) \subset B_{r_0}(x)$ and

$$\sup_{B_s(y) \cap \Sigma} |A|^2 \leq 4C^2 s^{-2} = 4|A|^2(y). \quad (15)$$

That is, the curvature at y is large (this just means that C should be thought of as a large constant equal to $s|A|(y)$) and is almost (up to the constant 4) the maximum on the ball $B_s(y)$. We will say that the pair (y, s) is a *blow up pair* and the point y is a *blow up point*. Later s will be replaced by $8s$ and eventually by a constant times s and sometimes the extrinsic ball will be replaced by an intrinsic ball, but we will still refer to the pair (y, s) as a blow up pair. That there exists such a point y is easy to see; on $B_{r_0}(x) \cap \Sigma$ set $F(z) = (r_0 - r(z))^2 |A|^2(z)$ where $r(z) = |z - x|$. Then

$$F(x) \geq 4C^2, F \geq 0, \text{ and } F|_{\partial B_{r_0}(x) \cap \Sigma} = 0. \quad (16)$$

Let y be where the maximum of F is achieved and set $s = C/|A|(y)$. Note that s is at most one-half of the distance from y to the boundary of the ball $B_{r_0}(x)$. One easily checks that y, s have the required properties. Namely, clearly $|A|^2(y) = C^2 s^{-2}$ and since y is where the maximum of F is achieved,

$$|A|^2(z) \leq \left(\frac{r_0 - r(y)}{r_0 - r(z)} \right)^2 |A|^2(y). \quad (17)$$

Since $F(x) \geq 4C^2$ it follows from the choice of s that $|r_0 - r(y)| \leq 2|r_0 - r(z)|$ for $z \in B_s(y) \cap \Sigma$. Hence, $|A|^2(z) \leq 4|A|^2(y)$. Together this gives (15).

The existence of multi-valued graphs is shown by combining a blow up result with an extension result. This blow up result says that if an embedded minimal disk in a ball has large curvature at a point, then it contains a small (in fact on the scale of $1/\max|A|$) almost flat N -valued graph nearby; this is A. in fig. 3. The extension result allows us to extend the (small) N -valued graphs almost out to the boundary of the “big” ball B_R ; this is B. in fig. 3. In fact, the blow up result shows that if (y, s) is a blow up pair with point y and radius $s > 0$ satisfying (15), then the corresponding N -valued function is defined on an annulus whose inner radius is s and so the initial separation is proportional to s . That is, for positive constants C_1, C_2

$$C_1 s \leq |w(s, \theta)| \leq C_2 s. \quad (18)$$

Equation (18) will be used implicitly in the next section.

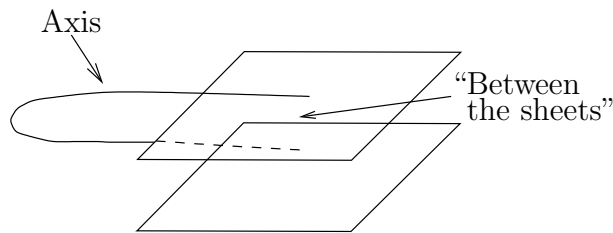


FIGURE 11. The curvature estimate “between the sheets.”

The extension result is significantly more subtle than the local existence of multi-valued graphs. The key for being able to extend is a curvature estimate “between the sheets” for embedded minimal disks; see fig. 11. We think of an axis for such a disk Σ as a point or curve away from which the surface locally (in an extrinsic ball) has more than one component. With this weak notion of an axis, the estimate between the sheets is that if one component of Σ is sandwiched between two others that connect to an axis, then there is a fixed bound for (the norm of) the curvature of the one that is sandwiched. The example to keep in mind is a helicoid and the components are “consecutive sheets” away from the axis. Once the estimate between the sheets is established, then it is applied to the “middle” sheet(s) of an N -valued graph to show that even as we go far out to the “outer” boundary of the N -valued graph the curvature has a fixed bound. Using this a priori bound and additional arguments one gets better bounds and eventually (with more work) argue that the sheets must remain almost flat and thus the N -valued graph will remain an N -valued graph.

The proof of the one-sided curvature estimate

Using a blow up argument and the minimal surface equation, one can show curvature estimates for minimal surfaces which on all sufficiently small scales lie on one side of, but come close to, a plane. Such an assumption is a scale invariant version of Theorem 2. However, the assumption of Theorem 2 is not scale invariant and the theorem cannot be proven this way. The scale invariant condition is very similar to the classical Reifenberg property. (A subset of \mathbf{R}^n has the Reifenberg property if it is close on all scales to a hyperplane; see the appendix of [ChC]. This property goes back to Reifenberg’s fundamental 1960

paper “Solution of the Plateau problem for m -dimensional surfaces of varying topological type”.) As explained above (in particular Corollary 1), the significance of Theorem 2 is indeed that it only requires closeness on one scale. On the other hand, this is what makes it difficult to prove (the lack of scale invariance is closely related to the lack of a useful monotone quantity).

Let us give a very rough outline of the proof of the one-sided curvature estimate; i.e., Theorem 2. Suppose that Σ is an embedded minimal disk in the half-space $\{x_3 > 0\}$ intersected with the ball B_{2r_0} and with boundary in the boundary of the ball B_{2r_0} . The curvature estimate is proven by contradiction; so suppose that Σ has low points with large curvature. Starting at such a point, we decompose Σ into disjoint multi-valued graphs using the existence of nearby points with large curvature (the existence of such nearby points is highly nontrivial to establish. We will use that such a nearby point of large curvature can be found below any given multi-valued graph and thus we can choose the “next” blow up point to always be below the previous). The key point is then to show (see Proposition 2 below) that we can in fact find such a decomposition where the “next” multi-valued graph starts off a definite amount below where the previous multi-valued graph started off. In fact, what we show is that this definite amount is a fixed fraction of the distance between where the two graphs started off. Iterating this eventually forces Σ to have points where $x_3 < 0$. This is the desired contradiction.

To show this key proposition (Proposition 2), we use two decompositions and two kinds of blow up points. The first decomposition uses the more standard blow up points given as pairs (y, s) where $y \in \Sigma$ and $s > 0$ is such that

$$\sup_{\mathcal{B}_{8s}(y)} |A|^2 \leq 4|A|^2(y) = 4C_1^2 s^{-2}. \quad (19)$$

(Here $\mathcal{B}_{8s}(y)$ is the intrinsic ball of radius $8s$, so in particular $\mathcal{B}_{8s}(y) \subset \Sigma$.) The point about such a pair (y, s) is that, since Σ is a minimal disk, Σ contains a multi-valued graph near y starting off on the scale s . (This is assuming that the curvature at y is sufficiently large, i.e., C_1 is a sufficiently large constant.) The second kind of blow up points are the ones where (except for a technical issue) 8 in the radius of the ball centered at y is replaced by some really large constant C , i.e.,

$$\sup_{\mathcal{B}_{Cs}(y)} |A|^2 \leq 4|A|^2(y) = 4C_1^2 s^{-2}. \quad (20)$$

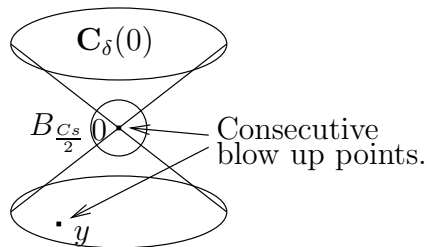


FIGURE 12. Two consecutive blow up points satisfying (20).

Proposition 2. (See fig. 12). There exists $\delta > 0$ such that if point 0, radius s satisfies (20) and $\Sigma_0 \subset \Sigma$ is the corresponding (to $(0, s)$) 2-valued graph over the annulus $D_{r_0} \setminus D_s$, then we get point y , radius t satisfying (20) with $y \in \mathbf{C}_\delta(0) \cap \Sigma \setminus B_{Cs/2}$ and where y is below Σ_0 .

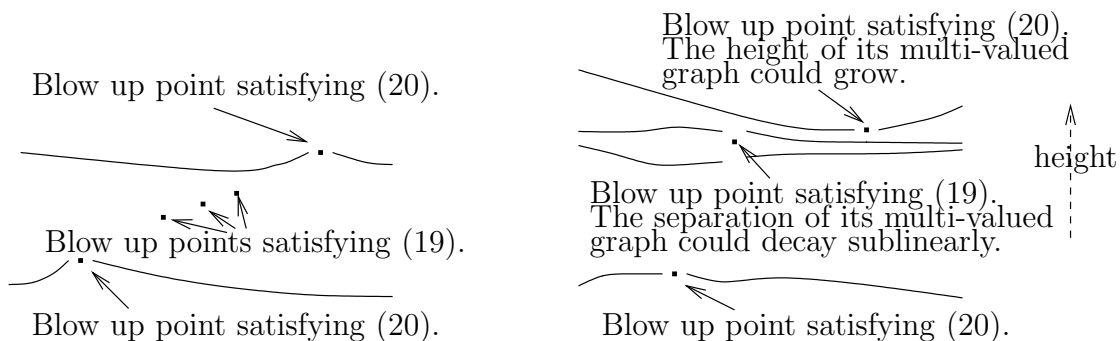


FIGURE 13. Between two consecutive blow up points satisfying (20) there are many blow up points satisfying (19).

FIGURE 14. Measuring height. Blow up points and corresponding multi-valued graphs.

The point for proving Proposition 2 is that we can find blow up points satisfying (20) so that the distance between them is proportional to the sum of the scales. Moreover, between consecutive blow up points satisfying (20), we can find many blow up points satisfying (19); see fig. 13. The advantage is now that if we look between blow up points satisfying (20), then the height of the multi-valued graph given by such a pair grows like a small power of the distance whereas the separation between the sheets in a multi-valued graph given by (19) decays (at the worst) like a small power of the distance; see fig. 14. Now, thanks to that the number of blow up points satisfying (19) (between two consecutive blow up points satisfying (20)) grows almost linearly, then, even though the height of the graph coming from the blow up point satisfying (20) could move up (and thus work against us), the sum of the separations of the graphs coming from the points satisfying (19) dominates the other term. Thus the next blow up point satisfying (20) (which lies below all the other graphs) is forced to be a definite amount lower than the previous blow up point satisfying (20). This gives the proposition.

Theorem 2 follows from the proposition. Suppose the theorem fails; starting at a point of large curvature and iterating the proposition will eventually give a point in the minimal surface with $x_3 < 0$, which is a contradiction.

Concluding remarks and some possible future directions of research

In this article we have seen that minimal surfaces and surfaces of “minimal” type occur naturally, and we have described why embedded minimal disks are double spiral staircases. We would hope that similar considerations can be used to answer, for other things than minimal disks, the age-old question:

“What are the possible shapes of various things and why?”.

A different possible direction is to describe 3-manifolds. Namely, by a result of B. White for a generic metric on a closed 3-manifold the area functional, that is, the map that to

each closed surface assigns its area, is a Morse function. (Recall that a Morse function is a function that only has nondegenerate critical points.) As we saw earlier, the critical points of the area functional are precisely the minimal surfaces; thus if one could understand all minimal surfaces in a given 3-manifold, M , then one would understand all critical points for the area functional. For a generic metric one could then hope to use Morse theoretic arguments to understand M . For general embedded minimal surfaces of a given fixed genus in closed 3-manifold, the key for understanding them is to understand their intersection with a small ball in M . Since locally any fixed 3-manifold is almost euclidean this boils down to understanding minimal surfaces in a ball in \mathbf{R}^3 with boundary in the boundary of the ball. The key for this is indeed the case where the minimal surfaces are disks, thus the key is the results described here. We will discuss this elsewhere.

The field of minimal surfaces has undergone enormous development since the days of Euler and Lagrange. It has played a key role in the development of many other fields in analysis and geometry. It has had times of intense development followed by times of stagnation before new fundamental results and techniques have been discovered. This has happened over and over again. In closing, we believe that, after nearly a quarter of a millenium, the field of minimal surfaces is at its very peak and of utmost importance in mathematics and its applications. We hope that this expository article has helped convey this. Although as the saying goes “it is hard to predict – especially about the future”¹, we believe that more magnificent results and techniques are to follow.

We are grateful to Christian Berg, Cornelius H. Colding, Chris Croke, Bruce Kleiner, Camillo De Lellis, Paul Schlapobersky, David Ussery, and David Woldbye for suggestions and comments, and we are particularly grateful to Andrew Lorent for his very many very helpful comments. Finally, we wish to thank the editor of the Notices of the AMS, Harold Boas, for his and the reviewer’s considerable help in making this article more readable.

REFERENCES

- [A] F.J. Almgren Jr, Minimal surface forms, *Math. Intelligencer*, 4 (1982) no. 4, 164–172.
- [ChC] J. Cheeger and T.H. Colding, On the Structure of Spaces with Ricci Curvature Bounded Below; I, *Jour. of Diff. Geometry* 46 (1997) 406-480.
- [C] T.H. Colding, The mathematics of double spiral staircases, in preparation.
- [CM1] T.H. Colding and W.P. Minicozzi II, Minimal surfaces, Courant Lecture Notes in Math., v. 4, 1999.
- [CM2] T.H. Colding and W.P. Minicozzi II, Embedded minimal disks, To appear in The Proceedings of the Clay Mathematics Institute Summer School on the Global Theory of Minimal Surfaces. MSRI. <http://www.arXiv.org/abs/math.DG/0206146>
- [CM3] T.H. Colding and W.P. Minicozzi II, Minimal surfaces in 3-manifolds, Graduate studies in Mathematics, AMS, in preparation.
- [CaDr] C.R. Calladine and H.R. Drew, Understanding DNA, Academic Press 1997.
- [DHKW] U. Dierkes, S. Hildebrandt, A. Kuster, O. Wohlrab, Minimal surfaces. I. and II., Grundlehren der Mathematischen Wissenschaften, 295 and 296. Springer-Verlag, Berlin, 1992.
- [K] W. Kahle, Color Atlas and textbook of human anatomy, vol. 3, Nervous system and sensory organs, Georg Thieme verlag, 3ed., 1986.
- [N] J.C.C. Nitsche, Lectures on minimal surfaces. Vol. 1. Introduction, fundamentals, geometry and basic boundary value problems. Cambridge University Press, Cambridge, 1989.
- [Op] J. Oprea, The mathematics of soap films: Explorations with Maple, AMS, Student Mathematical Library, vol. 10, 2000.

¹Quote attributed to Danish humorist Storm P. (Robert Storm Petersen) from the 1920s.

- [O] R. Osserman, A survey of minimal surfaces, Dover publications, inc. New York, 1986.
- [S] L. Simon, Survey lectures on minimal submanifolds, Seminar on minimal submanifolds, Ann. of Math. Stud., 103, Princeton Univ. Press, Princeton, NJ, 1983.
- [T] H.S. Tropp, Jesse Douglas, the Plateau problem, and the Fields Medal: some personal reflections. The problem of Plateau, 43–49, World Sci. Publishing, River Edge, NJ, 1992.

COURANT INSTITUTE OF MATHEMATICAL SCIENCES AND PRINCETON UNIVERSITY, 251 MERCER STREET,
NEW YORK, NY 10012 AND FINE HALL, WASHINGTON RD., PRINCETON, NJ 08544-1000

DEPARTMENT OF MATHEMATICS, JOHNS HOPKINS UNIVERSITY, 3400 N. CHARLES ST., BALTIMORE,
MD 21218

E-mail address: `colding@cims.nyu.edu`, `minicozz@jhu.edu`